Communicable Diseases Intelligence

2026 • Volume 50 • cdc.gov.au/cdi • Epub date: 29.09.2026 • doi.org/10.33321/cdi.2026.50.051

Enhancing influenza surveillance in Australia using Google search data combined with machine learning

Aminath Shausan, Adam G Dunn, Fiona J May, Satyamurthy Anuradha, Teresa M Wozniak, Amalie Dyda

Australian Centre for Disease Control

Communicable Diseases Intelligence

Communicable Diseases Intelligence (CDI) is a peer-reviewed scientific journal published by the Australian Centre for Disease Control.

The journal aims to disseminate information on the epidemiology, surveillance, prevention and control of communicable diseases of relevance to Australia and the near region.

Editor

Dr Elise Firman

Deputy Editor

Simon Petrie

Design and Production

Lisa Thompson

Editorial Advisory Board

David Durrheim, Mark Ferson, Clare Huppatz, John Kaldor, Martyn Kirk and Meru Sheel

Submit an Article

Submit your next communicable disease related article to CDI for consideration.

Guidelines for authors and details on how to submit your publication is available on our website, or by email to the CDI Editor.

Contact us

Communicable Diseases Intelligence (CDI)

Australian Centre for Disease Control

PO Box 795, Canberra ACT 2601

Australia

Website: **cdc.gov.au/cdi**

Email: **cdi.editor@cdc.gov.au**

© 2026 Commonwealth of Australia as represented by the Australian Centre for Disease Control

ISSN: 2209-6051 Online

This journal is indexed by Index Medicus and Medline.

Creative Commons Licence

This publication is licensed under a Creative Commons Attribution-Non-Commercial-NoDerivatives 4.0 International Licence (Licence). You must read and understand the Licence before using any material from this publication.

Restrictions

The Licence does not cover, and there is no permission given for, use of any of the following material found in this publication (if any):

- the Commonwealth Coat of Arms (by way of information, the terms under which the Coat of Arms may be used can be found on the Department of Prime Minister and Cabinet website);
- any logos (including the Australian Centre for Disease Control's logo) and trademarks;
- any photographs and images;
- any signatures; and
- any material belonging to third parties.

Disclaimer

Opinions expressed in *Communicable Diseases Intelligence* are those of the authors and not necessarily those of the Australian Government or the Australian Centre for Disease Control. Data may be subject to revision.

Enquiries

Enquiries regarding any other use of this publication should be addressed to the CDI Editor.

Contents

Abstract 4
Background 4
Methods 4
Results 4
Conclusion 4
Introduction 5
Materials and methods 5
Data 5
Modelling 6
Modelling scenarios 8
Evaluation measures 8
Results 9
Discussion 12
Code availability statement 13
Ethics statement 13
Financial support 13
Conflicts of interest 13
Author details 14
References 15
Appendix A: Summary of technical details for machine learning models 18
Appendix B: Assessment of machine learning model performance by jurisdiction 19

Original article

Abstract

Background

To effectively respond to acute respiratory infections such as influenza, timely information about the spread of disease is required. Surveillance methods that train machine learning models on Google Trends data have been developed to forecast outbreaks. Our aim was to examine the feasibility of forecasting influenza rates for states and territories in Australia using Google Trends data.

Methods

Weekly search volume data across 2018 and 2019 from Google Trends, for each state and territory in Australia excepting the Australian Capital Territory, were compared to weekly influenza notifications from the National Notifiable Disease Surveillance System (NNDSS). Four supervised machine learning regression models were developed: elastic net; support vector regression; random forest; and feedforward neural network. Models were fitted independently to data from each state and territory, considering nowcast (current week) and forecast (one and two weeks ahead) predictions.

Results

The results show that Google search volumes are correlated with reported influenza rates over time. Random forest and elastic net models generally showed better predictive performance compared to other models. Each modelled state and territory, except the Northern Territory and Tasmania, showed at least two search queries with moderate to strong Pearson correlation with the influenza notifications. The forecast accuracy (measured by the Pearson correlation coefficient) for the best-performing model varied by state or territory (from -0.353 to 0.977) and accuracy was lower for forecasts for one week and two weeks ahead.

Conclusion

Combinations of Google search data and machine learning showed predictive utility for forecasting weekly influenza rates in Australian jurisdictions, with lower accuracy in jurisdictions with smaller populations. Future work should investigate specific keywords by location exploring disease prediction at a more geographically specific level, with considerations for smaller populations and robustness over time.

Keywords: infectious diseases; influenza; machine learning; artificial intelligence; surveillance

Introduction

Acute respiratory infections cause considerable morbidity and mortality, as well as social and economic burden. In 2019 there were 313,033 notifications of laboratory-confirmed influenza in Australia, almost three times higher than the five-year average.[1] While the burden of disease due to influenza eased during the Australian COVID-19 pandemic response,[2,3] influenza transmission and disease burden has since returned to near pre-pandemic levels. There were 225,332 notifications of laboratory-confirmed influenza and 308 associated deaths in 2022,[4] and 252,296 notifications and 376 influenza associated deaths in 2023.[5]

The aim of surveillance is to provide detailed information about infectious disease incidence to inform public health planning and response, and to estimate future incidence as early as possible. Infectious disease surveillance in Australia relies predominantly on notifiable disease data which is collated in the National Notifiable Disease Surveillance System (NNDSS).[6] Currently, data collected in the NNDSS includes information on the number of notified cases, onset or specimen collection date as well as demographic information.[7]

Notification data collected at the state level is timelier and often more detailed than data collected by NNDSS, as automated notifications often come directly from the notifier (e.g. lab, clinician) and additional details can be collected during follow up, often with the case. States and territories collect identifying information under their relevant public health acts. However, as individual influenza cases are not routinely followed up, the state-level notification data is typically less detailed than for numerous other diseases. The influenza notification data which is currently available is considered an underestimate of the true burden of disease.[8] There are also a number of other influenza surveillance systems within Australia which collect data to enhance public health response, including FluTracking[9] and the Australian Sentinel Practice Research Network (ASPREN).[10]

New surveillance methods have emerged, using social media data and Google Trends in conjunction with machine learning (ML) models, to predict disease outbreaks.[11–14] Influenza surveillance using Google Trends data and ML models has been shown to be timelier in providing an early warning system.[12,15] Previous research has identified a number of key factors to develop the most accurate machine learning models for influenza prediction. This includes limiting keywords to those relevant to clinicians to reduce extraneous noise from internet data;[16] appropriate and complete outcome variables available; comprehensive data preprocessing; and creating additional variables to enhance model performance. The selection of modelling techniques is also important and can include decision trees, neural networks and support vector regression.[17–19]

The aim of this study was to compare the performance of several machine learning models for predicting future notified influenza rates using Google Trends data in Australian states and territories.

Materials and methods

Four forecasting regression models (elastic net; support vector regression; random forest; and feedforward neural network) were trained and evaluated for their predictive accuracy of influenza rates based on Google Trends data. The predictive accuracy was assessed using the mean absolute error, Pearson correlation coefficient, peak week difference, and peak magnitude difference between the estimated and actual influenza incidence rates.

Data

The data used in this study included a duration of 104 weeks from the first week of 2018 to the last week of 2019.

Publicly available state and territory level laboratory-confirmed weekly influenza notifications from the National Notifiable Disease Surveillance System (NNDSS) were used.[7] This dataset does not include data for the Australian Capital Territory. Thus, our analysis concerns influenza notifications for New South Wales, Victoria, Queensland, Western Australia, South Australia, Tasmania, and the Northern Territory. Based on the 2019 census,[20] the populations of the states and territories used in this study were:

- New South Wales: 8,166,401
- Victoria: 6,680,648
- Queensland: 5,184,847
- Western Australia: 2,639,222
- South Australia: 1,770,591
- Tasmania: 541,500
- Northern Territory: 245,929

We expect the number of influenza notifications would be higher for larger populations. The number of notifications per week was aggregated to represent the number of influenza cases that week. There were five missing weekly notifications in the Northern Territory. We assumed there were no influenza incidences in these five weeks for the Northern Territory and assigned 0 for those weeks. For consistency with Google Trends data, we scaled the influenza data for each jurisdiction to a range from 0 to 100.

We obtained Google search data from the Google Trends website,[i] a free tool with aggregated search volumes for user-submitted queries. Search volume is anonymised and normalised in comparison to all searches on the Google search engine for a given period, accounting for geolocation, category, and time frame. This normalisation scales the data from 0 to 100, with 0 and 100 corresponding to the lowest and highest search volumes, respectively, across the search period. Google Trends provides samples using real-time or retrospective data.[21]

We collected weekly retrospective search data for 22 influenza-related keywords from 1 January 2018 to 29 December 2019, for each of the seven Australian regions listed above. Keywords were selected based on prior influenza surveillance studies, which found that clinician-focused search terms outperform generic population search terms for detecting influenza activity and reducing noise from media coverage and seasonal variations.[16] Searches from the general population are more heavily impacted by media coverage and seasonal concern. Clinician search terms are more likely to be associated with real cases of disease as healthcare professionals are more likely to search for specific clinical presentations, treatment guidelines, or diagnostic criteria.

Without an established Australian methodology for identifying optimal influenza-related keywords, we used a keyword set previously shown to perform well in international surveillance studies and evaluated its applicability in the Australian context. The full list of search terms based on previous influenza surveillance research are available below in Table 1.

i https://trends.google.com/trends.

Table 1: Complete list of Google Trends search terms used

Keyword	References
Influenza	16, 22, 23
Tamiflu	16, 24, 25
Pneumonia	16, 23
Bronchitis	16, 24, 26
Flu	16, 23, 27
Rhinovirus	16, 24, 26
Haemophilus influenzae	16, 24, 26
Parainfluenza	16, 24, 26
H1N1	16, 23
H7N9	16, 23, 24
H5N1	16, 24
H3N2	16, 23
Grippe	16, 23
Gripe	16, 28
Adenovirus	16, 24, 26
Respiratory syncytial virus	16, 23, 24
Metapneumovirus	16, 24, 26
Bordetella pertussis	16, 24
Mycoplasma pneumoniae	16, 23, 24
H9N2	16, 23, 24
Sinusitis	16, 23, 24
Upper respiratory tract infection	16, 24, 26

Modelling

Initially, we performed correlation analysis by visually comparing the trends of state and territory level influenza rates and Google Trends data for each keyword. Subsequently, we applied Pearson correlation between the state and territory level influenza data and the corresponding Google Trends data to observe any significant positive correlation with the influenza rates. Four machine learning models for predicting influenza rates from Google Trends data were then developed. The models were fitted separately to each state and territory data. Below we detail the variables, models, experiments, and performance measures applied to investigate the predictive performance.

For each state and territory, the scaled weekly NNDSS influenza rate was used as the outcome variable. The weekly Google Trends search volume for each of 22 keywords corresponding to the geographic region of concern were considered as predictor variables.

1. **Elastic net regression:** a regularised linear regression technique that reduces overfitting by shrinking or eliminating unreliable predictors when predictors are highly correlated. This makes it useful for influenza forecasting from multiple related Google Trends search data, where multicollinearity is a frequent challenge. A crucial hyperparameter, l1_ratio, controls how much weight is given to the lasso (L1) compared to the ridge (L2) penalty. This is important as the balance between L1 and L2 penalties impacts which predictors are selected and how reliable the predictions are.[29–31]

2. **Support vector regression:** a kernel-based method that models complex nonlinear relationships by fitting a flexible function that minimises prediction error while maintaining model simplicity. Its ability to use kernel functions, such as radial basis or polynomial kernels, makes it well suited for influenza forecasting, where transmission dynamics often exhibit nonlinear patterns. Effective performance of the model depends on tuning key hyperparameters, including the kernel type and degree, the regularisation parameter, and the width of the ε-insensitive error zone, which together balance model flexibility to avoid both underfitting and overfitting.[32]

3. **Random forest regression:** an ensemble learning method that builds multiple decision trees, using bootstrapped samples and randomly selected predictors, then averages their predictions to reduce variance and improve prediction. Its ability to capture nonlinear relationships, predictor interactions, and complex epidemic dynamics, without relying on assumptions like linearity or normality makes it well suited for influenza forecasting and its robustness to multicollinearity further strengthens its utility. Key hyperparameters such as the number of trees and their maximum depth determine how the model balances bias and variance, with tuning ensuring that trees are neither too shallow nor too deep.[33]

4. **Feedforward neural network:** an artificial neural network that learns patterns by passing predictors through one or more hidden layers, where weighted combinations and nonlinear activation functions allow it to model flexible relationships between variables. This makes it well suited for influenza prediction, as it can capture complex epidemic patterns such as nonlinear trends, interactions between predictors, and delayed influences across weeks, particularly when patterns are too complex for linear models but the dataset is not large enough for deep architecture. Key hyperparameters such as regularisation strength and learning rate determine how smoothly and effectively the network learns, helping to prevent overfitting to short term or random variations in influenza incidence.[34]

We considered the four supervised machine learning methods detailed above to forecast weekly influenza rates.

These machine-learning models were chosen because they can capture complex, potentially nonlinear and multicollinear relationships in epidemiological time series while remaining practical to train on relatively small datasets, such as the weekly influenza rates analysed here. They do not rely on strong distributional assumptions, offering advantages over traditional statistical models when forecasting influenza activity. For the models based on support vector regression and feedforward neural network, we performed min-max scaling on the data to the range [0,1], ensuring these models can handle correlated predictors. As the temporal structure and small sample size of the data could cause unstable coefficient estimates, we performed temporally ordered cross-validated hyperparameter tuning to avoid overfitting and ensuring stable generalisation. The tuned hyperparameters for each model are described in Appendix A, Table A.1, and the temporal cross-validation strategy is detailed in the 'Modelling scenarios' section. We fitted these models applying the algorithms available from the Python *scikit-learn* library.[21]

Modelling scenarios

For each model we performed two types of predictions, those for the current week (nowcast) and predictions for one and two weeks into the future. For nowcasting we used Google Trends data from the current week (t) to predict notified influenza cases occurring in the same week (t). For the one and two week forecasts, we used Google Trends data from the current week (t) to predict influenza incidences occurring in the next week (t+1), and next two weeks (t+2), respectively.

For nowcast fitting, the first 83 weeks of data (80%) were used as the training set and the remaining 21 weeks (20%) as the test set. For the one and two weeks ahead forecasts, we kept the same 80% training set, but the test set was reduced by one or two weeks, respectively, to match the forecasting timeline. Hyperparameters were tuned within the training set using five-fold expanding-window temporal cross-validation with an eight-week validation horizon (see Appendix A, Figure A.1). This design respects time ordering of the data and eliminates information leakage from the past into the future and is best suited for time-series forecasting. The optimal settings were chosen based on the average validation error across folds, after which each model was refitted on the full training set and evaluated once on the test set. All transformation and scaling steps were performed within the training folds only, ensuring that information leakage did not bias model evaluation. Evaluation measures applied to measure model performance are described in the next section.

Evaluation measures

Model performance was assessed on the test set only, ensuring an unbiased estimate of out-of-sample forecast ability. We used four complementary measures comparing the predicted and actual influenza rates: mean absolute error; Pearson correlation coefficient; peak week difference; and peak magnitude difference.

The mean absolute error measures point-forecast accuracy and is robust to outliers. It is computed as the absolute difference between actual and predicted values. The Pearson correlation coefficient measures how closely the predicted and actual values follow the same epidemiological pattern or trend. A lower mean absolute error means fewer errors, while a higher Pearson correlation coefficient means better alignment between predictions and actual influenza rates. These measures are not comparable; however, lower values of the mean absolute error and higher values of the Pearson correlation coefficient each indicate better predictive accuracy.

We calculated the difference between the actual and predicted weeks when the highest number of cases occurred during the forecasted period, known as the peak week difference, as well as the peak magnitude difference or difference between actual and predicted height of the peak. The peak week difference and peak magnitude difference assess accuracy of predicted epidemic timing and severity, respectively. Lower peak week difference and peak magnitude difference values indicate better model performance. However, not all regions showed a clear peak in influenza cases during the forecast period. As a result, we only calculated peak week difference and peak magnitude difference in cases where a peak was visible in the data or when the model predicted a peak during the forecast period.

To select the best model, we compared the mean absolute error followed by Pearson correlation coefficient of each model. If there were major or minor peaks in the test set, the peak week difference and peak magnitude difference measures were applied. Using multiple metrics captures different aspects of forecasting performance and reduces the risk of overinterpreting results based on a single criterion. As random forest and elastic net models can identify the variables most important for making predictions, these variables were ranked by importance and visual plots created. For the random forest model, the ranking graph shows a cumulative importance curve, which highlights how much each variable contributes to the model's overall predictions. The curve's maximum value is 1 and variables were considered important if the contribution to the cumulative importance was < 0.95. For the elastic net models, the ranking graph displays the absolute value of each variable's coefficient (a measure of its impact on predictions). Variables were considered important if their coefficient was > 0.1. The purpose of selecting important variables was to add context and validity to the study, rather than assess model performance.

Further detail on the implementation and validation of the models used is provided in the Supplementary information for this article.

Results

In an example indicating the correlation between Google Trends data and influenza rates, there is a similar pattern for searches of 'influenza' and influenza rates in Queensland (Figure 1). With the exceptions of the Northern Territory and Tasmania, the influenza rate for each region showed moderate to strong Pearson correlation ($r \geq 0.5$, $p \leq 0.05$) with at least two keywords (Table 2).

The analysis identified differences in keyword relevance across regions, with the keywords *influenza*, *Tamiflu* and *pneumonia* selected as consistent predictors of influenza across several states and territories (Table 2).

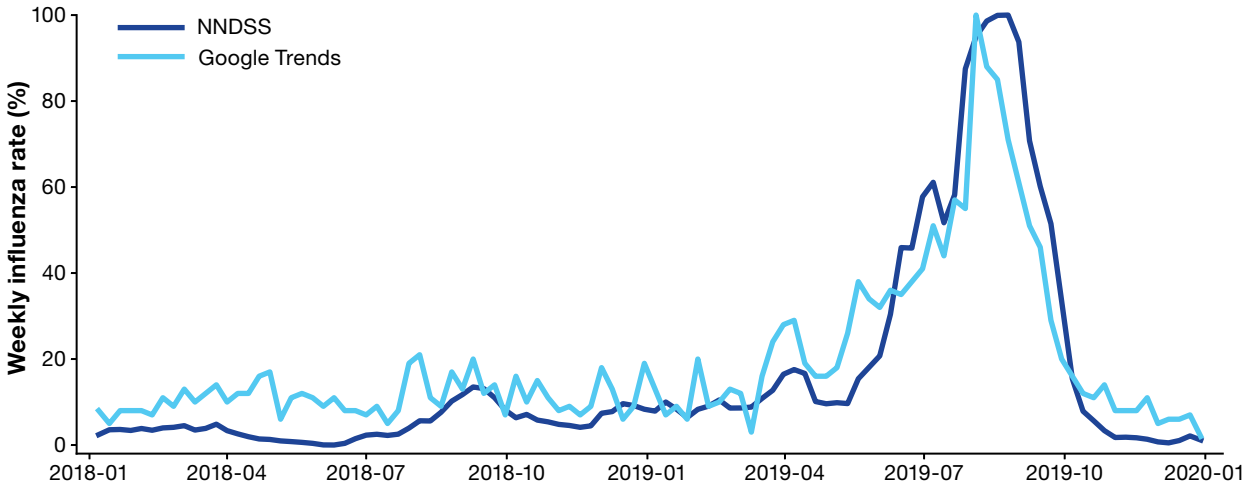
Results showed significant variation across models for the three types of prediction (nowcast, one and two weeks ahead forecasts) across regions (Appendix B, Figures B.1 – B.7). The elastic net model produced the best results in New South Wales, Victoria, Queensland and Western Australia for the nowcast prediction (Table 3). The random forest models produced the best results in New South Wales, Victoria, South Australia and Tasmania for one-week ahead predictions. For this same prediction type, the elastic net model produced the best results for Queensland (Table 4). For predictions two weeks ahead, random forest was the highest performing model in most states, except for Queensland in which the elastic net regression was the highest performing model. The support vector model was the highest performing model in South Australia for the two weeks ahead predictions (Table 5).

The nowcast predictions (Table 3) had the lowest mean absolute error and highest Pearson correlation coefficient compared to the results for one (Table 4) and two weeks ahead forecasts (Table 5). This implies that the nowcast prediction type most accurately estimated the actual influenza rates and closely captured the actual trend. The predictions for two weeks ahead generally had higher mean absolute error across most states, indicating that the accuracy declined over time.

States with larger populations (New South Wales, Queensland and Victoria) showed consistently better predictions, with higher Pearson correlation coefficient, than smaller population states and territories. The nowcast predictions were also accurate in Western Australia; however, there were differences in peak week and magnitude. Northern Territory and Tasmania results had lower or negative Pearson correlation coefficient, indicating lower-performing predictions.

Similarly, the models were able to better predict the time and peak magnitude of influenza cases for states with large populations (Queensland and New South Wales). For both states the nowcast models produced lower peak week difference and peak magnitude difference, which shows higher similarity between the actual and predicted influenza rates for the peak timing and magnitude. Among best-performing models by jurisdiction, Tasmania had the highest peak magnitude difference results (nowcast: 68.32, Table 3; one week ahead: 72.41, Table 4).

Figure 1: Comparison of Google Trends data for the keyword 'influenza' and National Notifiable Diseases Surveillance System (NNDSS) influenza rates for Queensland, Australia,[a] for the period January 2018 – December 2019



a NNDSS influenza notifications for the period January 2018 – December 2019 were scaled to a peak of 100 to allow comparison with the equivalently scaled Google Trends data.

Table 2: Pearson correlation coefficient between Google Trends data and National Notifiable Diseases Surveillance System (NNDSS) influenza rates, by jurisdiction and keyword,[a] January 2018 – December 2019, Australia

	Pearson correlation coefficient by jurisdiction[b]						
Keyword	**NSW**	**Vic.**	**Qld**	**WA**	**SA**	**NT**	**Tas.**
influenza	0.94	0.90	0.94	0.92	0.90	0.051	0.28
Tamiflu	0.89	0.69	0.72	0.59	0.40	-0.005	-0.016
pneumonia	0.72	0.63	0.56	0.58	0.28	0.16	0.23
bronchitis	0.43	0.60	0.36	0.29	-0.017	0.14	0.14
flu	0.39	0.43	0.31	0.75	0.86		0.33
rhinovirus	0.44	0.035	0.41	0.097	-0.04	0.022	-0.12
Haemophilus influenzae	-0.03	0.13	0.038	0.13	0.036		
parainfluenza	0.14	0.17	0.014	0.093	0.017		0.053
H1N1	0.067	0.1	-0.079	-0.016	0.0043	-0.078	-0.061
H7N9	0.032	-0.027	-0.16	-0.035	0.081		-0.098
H5N1	0.17	-0.085	0.004	-0.075	0.12		-0.037
H3N2	0.037	-0.087	-0.083	-0.13	-0.028		
grippe	-0.14	0.023	0.047	0.017	-0.12		
gripe	0.17	-0.048	0.15	0.071	0.063		0.025
adenovirus	0.21	0.05	0.2	0.018	0.063		-0.11
respiratory syncytial virus	0.072	-0.17	0.016	-0.11	0.21		-0.054
metapneumovirus	-0.074	0.026	0.033	-0.0016	-0.11		0.077
Bordetella pertussis	0.099	-0.067	0.033				
Mycoplasma pneumoniae	-0.1	0.19	0.015	-0.087	-0.088		
H9N2		-0.043					
sinusitis	0.17	0.13	0.21	0.14	-0.022		-0.23
upper respiratory tract infection	-0.012	0.0067	0.047	-0.13	0.14		



a This table provides a heat map, by jurisdiction and keyword, of the Pearson correlation coefficient (PCC) between Google Trends keyword data and the scaled NNDSS influenza rate. Cells highlighted in blue indicate significant correlation (PCC ≥ 0.5) for this jurisdiction and keyword; cells shaded grey represent PCC values < 0.5 for the jurisdiction/keyword combination; cells left blank indicate where no searches were performed for the corresponding keyword in the indicated jurisdiction.

b NSW: New South Wales; Vic.: Victoria; Qld: Queensland; WA: Western Australia; SA: South Australia; NT: Northern Territory; Tas.: Tasmania.

Table 3: Optimal model for nowcast Google Trends influenza prediction by jurisdiction,[a] Australia, January 2018 – December 2019

Jurisdiction	Best model	Mean absolute error	Pearson correlation coefficient	Peak week difference[b]	Peak magnitude difference[b]	Population (2019)
New South Wales	Elastic net	5.16	0.97	2	-8.90	8,166,401
Victoria	Elastic net	8.42	0.96	1	13.24	6,680,648
Queensland	Elastic net	7.76	0.98	2	5.07	5,184,847
Western Australia	Elastic net	3.28	0.91	N/A	N/A	2,639,222
South Australia	Random forest	4.90	0.34	4	-4.87	1,770,591
Tasmania	Elastic net	22.41	0.53	-2	68.32	541,500
Northern Territory	Random forest	7.25	-0.19	6	-9.86	245,929

a This table shows the best-performing model of the four machine learning models (elastic net; support vector; random forest; and feedforward neural network), and the model's performance measures (mean absolute error; Pearson correlation coefficient; peak week difference; and peak magnitude difference) based on the nowcast prediction type for each Australian jurisdiction except the Australian Capital Territory. The performance of the best model for each jurisdiction is compared with its population for 2019.

b N/A: not applicable, indicating no peak was available for the forecasted period.

Table 4: Optimal model for one-week-ahead Google Trends influenza prediction by jurisdiction,[a] Australia, January 2018 – December 2019

Jurisdiction	Best model	Mean absolute error	Pearson correlation coefficient	Peak week difference[b]	Peak magnitude difference[b]	Population (2019)
New South Wales	Random forest	4.36	0.96	-2	2.84	8,166,401
Victoria	Random forest	7.01	0.94	0	-10.24	6,680,648
Queensland	Elastic net	5.48	0.99	2	-16.55	5,184,847
Western Australia	Elastic net	3.63	0.84	N/A	N/A	2,639,222
South Australia	Random forest	6.62	-0.06	-9	-7.72	1,770,591
Tasmania	Random forest	19.91	0.35	1	72.41	541,500
Northern Territory	Random forest	8.00	-0.27	5	-12.59	245,929

a This table shows the best-performing model of the four machine learning models (elastic net; support vector; random forest; and feedforward neural network), and the model's performance measures (mean absolute error; Pearson correlation coefficient; peak week difference; and peak magnitude difference) based on the one-week-ahead prediction type for each Australian jurisdiction except the Australian Capital Territory. The performance of the best model for each jurisdiction is compared with its population for 2019.

b N/A: not applicable, indicating no peak was available for the forecasted period.

Table 5: Optimal model for two-weeks-ahead Google Trends influenza prediction by jurisdiction,[a] Australia, January 2018 – December 2019

Jurisdiction	Best model	Mean absolute error	Pearson correlation coefficient	Peak week difference[b]	Peak magnitude difference[b]	Population (2019)
New South Wales	Random forest	8.13	0.87	-3	-7.16	8,166,401
Victoria	Random forest	6.35	0.93	-1	-4.48	6,680,648
Queensland	Elastic net	12.19	0.98	1	-24.10	5,184,847
Western Australia	Elastic net	3.36	0.85	N/A	N/A	2,639,222
South Australia	Support vector	4.65	0.34	-5	4.978	1,770,591
Tasmania	Random forest	16.27	0.41	0	54.28	541,500
Northern Territory	Random forest	7.94	-0.35	4	-7.51	245,929

a This table shows the best-performing model of the four machine learning models (elastic net; support vector; random forest; and feedforward neural network), and the model's performance measures (mean absolute error; Pearson correlation coefficient; peak week difference; and peak magnitude difference) based on the two-weeks-ahead prediction type for each Australian jurisdiction except the Australian Capital Territory. The performance of the best model for each jurisdiction is compared with its population for 2019.

b N/A: not applicable, indicating no peak was available for the forecasted period.

Discussion

In an evaluation of machine learning models that use Google Trends data to forecast influenza rates in Australia, models typically performed better for larger populations and for more immediate predictions (nowcast) compared to further in the future (one and two weeks ahead). Overall, the random forest and elastic net models were the most effective models when properly adjusted for hyperparameters.

For most states or territories in Australia, machine learning models produced reasonably accurate influenza predictions for nowcasting as well as for predictions up to two weeks in advance. The search volume for many keywords correlates proportionally with notified influenza cases. The prediction of outbreaks up to two weeks earlier than conventional surveillance methods, such as the notification data used to train the model, is consistent with previous work.[35] Analysis with publicly available Google Trends data has shown that this type of influenza forecasting can be more timely than traditional methods.[21] Research in the Australian context has provided timeliness of 3–4 weeks, which may suggest the need to include more traditional models into this work such as susceptible-exposed-infectious-removed (SEIR) models, as well as more data (i.e., more broad keywords) to improve this current model.[36]

The usefulness of Google Trends data for predicting influenza notifications was less conclusive for the Northern Territory and Tasmania, likely due to lower populations in these jurisdictions. The Northern Territory and Tasmania seasonality also differs from the rest of the country. To be useful for surveillance, data needs to be localised, yet national influenza news may increase local searches. These findings highlight the influence of population size and regional seasonality on predictive accuracy. Future studies could consider including more broad search terms which are more likely to be used by the public.

The keywords *influenza* and *flu* were important predictors across several regions (Figure A.8). However, there were also differences in keywords by region. This highlights the importance of location specific data and predictions when this method is used within Australia. For example, searches including the keyword *rhinovirus* held significance in Queensland and Tasmania only, which may result from symptoms that overlap with influenza. The influenza season usually coincides with other respiratory diseases such as rhinovirus. Because of this, selection of keywords is important and requires further investigation.

In this study, we limited keywords to those that are most relevant to clinicians to reduce extraneous noise from internet data and to enhance the specificity of search analyses.[37] However, as this analysis identified search volume as an issue, future work may benefit from considering additional location-specific search terms. Furthermore, refining predictive models requires a better understanding of the relationship between respiratory illness and search behaviours and the complex factors that influence them.

There are several limitations in this study which need to be considered. A key limitation is the short time frame used for model testing. Data from the end of the influenza season was used, when notifications were declining so the model has not yet been tested using an entire influenza season or to predict the peak of a season. Hence, the model performance primarily shows the ability to identify short-term temporal variations. In addition, the keywords used were based on prior international research to assess evaluate known methods within the Australian context. This study did not compare alternative keyword groups, hence future work will require evaluation of the most appropriate key words. Notification data introduces selection bias, as only those who undergo testing get notified. For example, point-of-care testing is increasing, but results are not currently notifiable, which may decrease the accuracy of notification data over time. Despite these limitations, previous work has shown that trends are comparable using the notification data.[8] We used relative search volume and not absolute search phrase volume, reflecting the expectation that search volume is relative to other keywords and may be influenced by social and media trends. The analysis also does not capture those who do not use Google; data shows that different demographics use different search engines.[38,39] Despite these limitations, the findings show a proof of concept for the feasibility of using Google Trends data to identify increasing influenza activity within the Australian context, providing a baseline for future robust assessment.

There are also important digital data biases to consider. Online search behaviour is influenced by demographics, events in the media and access to the internet.[40] To minimise this bias, clinically specific keywords were used to avoid influence from media coverage. However, these data are unlikely representative as specific groups, such as older adults and those with lower digital literacy, are less likely to access online searching. In addition, the search behaviour of the population changes over time.[41] We did not include lagged influenza rates as a predictor along with Google Trends data, as our aim was to establish the Google Trends data's predictive ability for influenza surveillance in Australia. We anticipate that including lagged influenza rates can capture autocorrelation and may provide better predictive performance across all models. Future research should include lagged influenza rates in the models. The introduction of large language models such as ChatGPT has changed online searching behaviour. These tools are increasingly being used as alternatives to Google which could impact future use of these data.[42] The type of health searches may also change as the new tools provide a conversational format. These changes highlight the need for digital public health tools to adapt to changing digital information systems.

Google Trends data is a credible data source to detect increases in influenza cases, in addition to traditional surveillance for regions with higher populations. These findings may have implications for public health surveillance. These types of models may be able to supplement current surveillance methods by providing an early warning signal. Notification data and other routinely collected data sources will likely provide more detailed epidemiological data. However, using search data and machine learning to identify increases in influenza activity early can support a timely public health response. Future research should investigate specific keywords by location, exploring disease prediction at a more geographically specific level, with considerations for smaller populations and robustness over time.[43]

Code availability statement

All code required for modelling and analysis of this manuscript is available from GitHub (https://github.com/aminathshausan/Digital-Disease-Surveillance)

Ethics statement

Ethics approval for this study was provided by The University of Queensland Human Research Ethics Committee (2022/HE000173). All data used were anonymised and aggregate, with no individual-level data accessed or linked.

Financial support

We gratefully acknowledge funding provided by the School of Public Health, The University of Queensland.

Conflicts of interest

None to declare.

Author details

Dr Aminath Shausan,[1]

Prof. Adam G Dunn,[2]

Dr Fiona J May,[3]

Dr Satyamurthy Anuradha,[4,5]

A/Prof. Teresa M Wozniak,[1]

Dr Amalie Dyda[5]

1. Australian e-Health Research Centre CSIRO, Brisbane, Queensland, Australia
2. Faculty of Medicine and Health, University of Sydney, Sydney, Australia
3. Gold Coast Public Health Unit, Gold Coast Hospital and Health Service, Queensland, Australia
4. Metro South Public Health Unit, Metro South Health, Brisbane, Queensland, Australia
5. School of Public Health, University of Queensland, Queensland, Australia

Corresponding author

Dr Aminath Shausan

Level 7, 296 Herston Road, STARS Building, Herston Qld 4029

Phone: +61 7 3253 3627

Email: aminath.shausan@csiro.au

References

1. Australian Government Department of Health, Disability and Ageing. *2019 Influenza Season in Australia: A summary from the National Influenza Surveillance Committee*. Canberra: Australian Government Department of Health, Disability and Ageing; 30 June 2021. [Accessed on 2 February 2024.] Available from: https://www.health.gov.au/sites/default/files/documents/2022/10/aisr-2019-national-influenza-season-summary.pdf.

2. Adegbija O, Walker J, Smoll N, Khan A, Graham J, Khandaker G. Notifiable diseases after implementation of COVID-19 public health prevention measures in Central Queensland, Australia. *Commun Dis Intell (2018)*. 2021;45. doi: https://doi.org/10.33321/cdi.2021.45.11.

3. Bhatt P, Strachan J, Easton M, Franklin L, Drewett G. Effect of COVID-19 restrictions and border closures on vaccine preventable diseases in Victoria, Australia, 2020–2021. *Commun Dis Intell (2018)*. 2022;45. doi: https://doi.org/10.33321/cdi.2022.46.29.

4. Australian Government Department of Health, Disability and Ageing. *National 2022 Influenza Season Summary*. Canberra: Australian Government Department of Health, Disability and Ageing; December 2022. [Accessed on 2 February 2024.] Available from: https://www.health.gov.au/sites/default/files/2022-12/aisr-2022-national-influenza-season-summary.pdf.

5. Communicable Disease Epidemiology and Surveillance Section (CDESS). *Australian Influenza Surveillance Report – 2023 End of Season Summary*. Canberra: Australian Government Department of Health, Disability and Ageing; December 2023. [Accessed on 2 February 2024.] Available from: https://www.health.gov.au/sites/default/files/2023-12/aisr-2023-national-influenza-season-summary.pdf.

6. Australian Government Federal Register of Legislation. *National Health Security (National Notifiable Disease List) Instrument 2018*. [Legislation.] Canberra: Australian Government; 1 January 2025. [Accessed on 2 February 2025.] Available from: https://www.legislation.gov.au/F2018L00450/latest/text.

7. Australian Centre for Disease Control (Australian CDC). National Notifiable Diseases Surveillance System (NNDSS). [Webpage.] Canberra: Australian CDC; 28 January 2026. Available from: https://www.cdc.gov.au/diseases/surveillance-systems-and-networks/national-notifiable-diseases-surveillance-system-nndss.

8. Muscatello DJ, Amin J, Raina MacIntyre CR, Newall AT, Rawlinson WD, Sintchenko V et al. Inaccurate ascertainment of morbidity and mortality due to influenza in administrative databases: a population-based record linkage study. *PloS One*. 2014;9(5);e98446. doi: https://doi.org/10.1371/journal.pone.0098446.

9. Dalton C, Durrheim D, Fejsa J, Francis L, Carlson S, d'Espaignet ET et al. Flutracking: a weekly Australian community online survey of influenza-like illness in 2006, 2007 and 2008. *Commun Dis Intell Q Rep*. 2009;33(3);316–22. doi: https://doi.org/10.33321/cdi.2009.33.34.

10. Chilver M, Blakeley D, Stocks N. The Australian Sentinel Practices Research Network, 1 January to 31 March 2017. *Commun Dis Intell Q Rep*. 2017;41(4):E492–6. doi: https://doi.org/10.33321/cdi.2017.41.51.

11. Sooknanan J, Mays N. Harnessing social media in the modelling of pandemics—challenges and opportunities. *Bull Math Biol*. 2021;83(5);57. doi: https://doi.org/10.1007/s11538-021-00895-3.

12. Chu AM, Chong ACY, Lai NHT, Tiwari A, So MKP. Enhancing the predictive power of Google trends data through network analysis: infodemiology study of COVID-19. *JMIR Public Health Surveill*. 2023;9:e42446. doi: https://doi.org/10.2196/42446.

13. Santangelo OE, Gentile V, Pizzo S, Giordano D, Cedrone F. Machine learning and prediction of infectious diseases: a systematic review. *Mach Learn Knowl Extr*. 2023;5(1);175–98. doi: https://doi.org/10.3390/make5010013.

14. Wang A, Dara R, Yousefinaghani S, Maier E, Sharif S. A review of social media data utilization for the prediction of disease outbreaks and understanding public perception. *Big Data Cogn Comput*. 2023;7(2);72. doi: https://doi.org/10.3390/bdcc7020072.

15. Farhadloo M, Winneg K, Chan MPS, Jamieson KH, Albarracin D. Associations of topics of discussion on Twitter with survey measures of attitudes, knowledge, and behaviors related to Zika: probabilistic study in the United States. *JMIR Pub Health Surveill*. 2018;4(1):e16. doi: https://doi.org/10.2196/publichealth.8186.

16. Santillana M, Nsoesie EO, Mekaru SR, Scales D, Brownstein JS. Using clinicians' search query data to monitor influenza epidemics. *Clinic Infect Dis*. 2014;59(10);1446–50. doi: https://doi.org/10.1093/cid/ciu647.

17. McCoy D, Mgbara W, Horvitz N, Getz WM, Hubbard A. Ensemble machine learning of factors influencing COVID-19 across US counties. *Sci Rep*. 2021;11(1):11777. doi: https://doi.org/10.1038/s41598-021-90827-x.

18. Kumar R, Maheshwari S, Sharma A, Linda S, Kumar S, Chatterjee I. Ensemble learning-based early detection of influenza disease. *Multimed Tools Appl*. 2024;83(2);5723–43. doi: https://doi.org/10.1007/s11042-023-15848-2.

19. Lu FS, Hou S, Baltrusaitis K, Shah M, Leskovec J, Sosic R et al. Accurate influenza monitoring and forecasting using novel internet data streams: a case study in the Boston metropolis. *JMIR Pub Health Surveill*. 2018;4(1);e4. doi: https://doi.org/10.2196/publichealth.8950.

20. Australian Bureau of Statistics (ABS). National, state and territory population. Reference period: December 2019. [Internet.] Canberra: ABS; 18 June 2020. [Accessed on 2 February 2024.] Available from: https://www.abs.gov.au/statistics/people/population/national-state-and-territory-population/dec-2019#:~:text=Australia's%20population%20was%2025%2C522%2C169%20people,due%20to%20net%20overseas%20migration.

21. Kandula S, Shaman J. Reappraising the utility of Google flu trends. *PLoS Comput Biol*. 2019;15(8);e1007258. doi: https://doi.org/10.1371/journal.pcbi.1007258.

22. Choi SB, Kim J, Ahn I. Forecasting type-specific seasonal influenza after 26 weeks in the United States using influenza activities in other countries. *PLoS One*. 2019;14(11):e0220423. doi: https://doi.org/10.1371/journal.pone.0220423.

23. Zhang Y, Yakob L, Bonsall MB, Hu W. Predicting seasonal influenza epidemics using cross-hemisphere influenza surveillance data and local internet query data. *Sci Rep*. 2019;9(1):3262. doi: https://doi.org/10.1038/s41598-019-39871-2.

24. Lampos V, Miller AC, Crossan S, Stefansen C. Advances in nowcasting influenza-like illness rates using search query logs. *Sci Rep*. 2015;5(1):12760. doi: https://doi.org/10.1038/srep12760.

25. Cho S, Sohn CH, Jo MW, Shin S-Y, Lee JH, Ryoo SM et al. Correlation between national influenza surveillance data and Google trends in South Korea. *PLoS One*. 2013;8(12):e81422. doi: https://doi.org/10.1371/journal.pone.0081422.

26. Yang S, Santillana M, Kou SC. Accurate estimation of influenza epidemics using Google search data via ARGO. *Proc Natl Acad Sci U S A*. 2015;112(47):14473–8. doi: https://doi.org/10.1073/pnas.1515373112.

27. Ginsberg J, Mohebbi MH, Patel RS, Brammer L, Smolinski MS, Brilliant L. Detecting influenza epidemics using search engine query data. *Nature*. 2009;457(7232):1012–4. doi: https://doi.org/10.1038/nature07634.

28. Pelat C, Turbelin C, Bar-Hen A, Flahault A, Valleron A. More diseases tracked by using Google Trends. *Emerg Infect Dis*. 2009;15(8):1327–8. doi: https://doi.org/10.3201/eid1508.090299.

29. Tibshirani R. Regression shrinkage and selection via the lasso. *J R Statist Soc B*. 1996;58(1):267–88. doi: https://doi.org/10.1111/j.2517-6161.1996.tb02080.x.

30. Hoerl AE, Kennard RW. Ridge regression: biased estimation for nonorthogonal problems. *Technometrics*. 1970;12(1):55–67. doi: https://doi.org/10.1080/00401706.1970.10488634.

31. Zou H, Hastie T. Regularization and variable selection via the elastic net. *J R Stat Soc Ser B Stat Methodol*. 2005;67(2);301–20. doi: https://doi.org/10.1111/j.1467-9868.2005.00503.x.

32. Smola AJ, Schölkopf B. A tutorial on support vector regression. *Stat Comput*. 2004;14;199–222. doi: https://doi.org/10.1023/B:STCO.0000035301.49549.88.

33. Breiman L. Random forests. *Mach Learn*. 2001;45;5–32. doi: https://doi.org/10.1023/A:1010933404324.

34. Svozil D, Kvasnicka V, Pospichal J. Introduction to multi-layer feed-forward neural networks. *Chemom Intell Lab Syst*. 1997;39(1);43–62. doi: https://doi.org/10.1016/S0169-7439(97)00061-0.

35. Milinovich GJ, Williams GM, Clements ACA, Hu W. Internet-based surveillance systems for monitoring emerging infectious diseases. *Lancet Inf Dis*. 2014;14(2);160–8. doi: http://dx.doi.org/10.1016/S1473-3099(13)70244-5.

36. Moss R, Zarebski A, Dawson P, McCaw JM. Retrospective forecasting of the 2010–2014 Melbourne influenza seasons using multiple surveillance systems. *Epidemiol Infect*. 2017;145(1):156–69. doi: https://doi.org/10.1017/S0950268816002053.

37. Kurian SJ, Bhatti AUR, Alvi MA, Ting HH, Storlie C, Wilson PM et al. Correlations between COVID-19 cases and google trends data in the United States: a state-by-state analysis. *Mayo Clin Proc*. 2020;95(11);2370–81. doi: https://doi.org/10.1016/j.mayocp.2020.08.022.

38. Fergie G, Hilton S, Hunt K. Young adults' experiences of seeking online information about diabetes and mental health in the age of social media. *Health Expect*. 2016;19(6);1324–35. doi: https://doi.org/10.1111/hex.12430.

39. Vogels EA, Gelles-Watnick R. Teens and social media: Key findings from Pew Research Center surveys. [Webpage.] Washington DC: Pew Research Center; 24 April 2023. Available from: https://www.pewresearch.org/short-reads/2023/04/24/teens-and-social-media-key-findings-from-pew-research-center-surveys/.

40. Aiello AE, Renson A, Zivich PN. Social media- and internet-based disease surveillance for public health. *Annu Rev Public Health*. 2020;41:101–18. doi: https://doi.org/10.1146/annurev-publhealth-040119-094402.

41. Bachl M, Link E, Mangold F, Stier S. Search engine use for health-related purposes: behavioral data on online health information-seeking in Germany. *Health Commun*. 2024;39(8):1651–64. doi: https://doi.org/10.1080/10410236.2024.2309810.

42. Xu R, Feng Y, Chen H. ChatGPT vs. Google: a comparative study of search performance and user experience. *arXiv*. 2023. doi: https://doi.org/10.48550/arXiv.2307.01135.

43. Lazer D, Kennedy R, King G, Vespignani A. Big data. The parable of Google Flu: traps in big data analysis. *Science*. 2014;343(6176);1203–5. doi: https://doi.org/10.1126/science.1248506.

Appendix A: Summary of technical details for machine learning models

In this section, we describe the tuned hyperparameters and their values and illustrate the five-fold expanding window temporal cross-validation framework. Table A.1 lists the hyperparameters tuned for each model, along with their values tested.

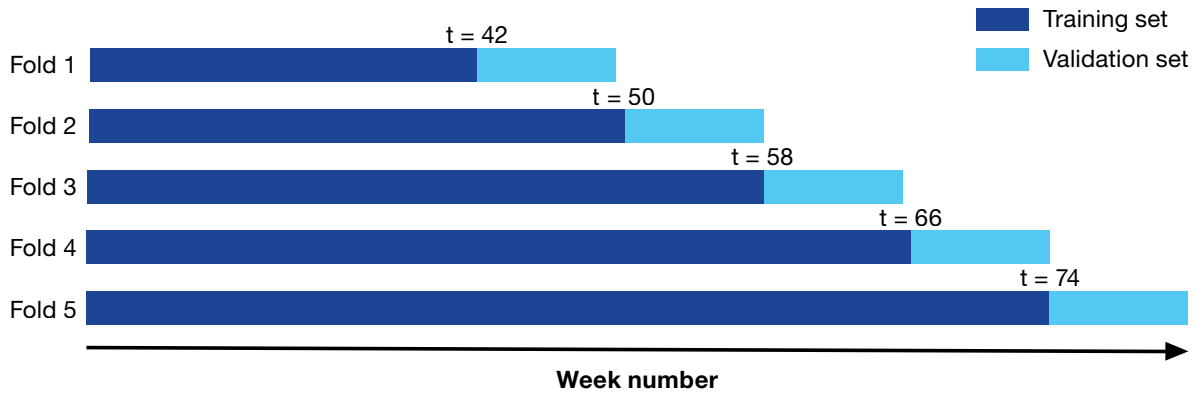
Table A.1: Tuned hyperparameters for each model, along with their value ranges/choices tested

Model	Hyperparameters tuned and their value range/choice
Elastic net regression	*l1_ratio*: from 0 to 1
Support vector regression	*kernel*: linear, radial, polynomial, and sigmoid; *degree*: from 1 to 3; *C* (regularisation parameter): from 0.001 to 10,000; *epsilon* (width of ε-insensitive error zone): from 0.0001 to 1.1
Random forest regression	*n_estimators* (number of trees): from 50 to 150; *max_depth* (maximum depth): from None to 20
Feedforward neural network[a]	*alpha* (regularisation parameter): from 0.0001 to 1; *learning_rate*: constant, adaptive

a For each Feedforward neural network model fit, we used three hidden layers with sizes *n*, 50, and 25, where *n* is the number of predictors, with *relu* activation function, *adam* optimiser and 1000 iterations. Early stopping was applied to terminate training when validation score was not improving.

Figure A.1 illustrates the 5-fold expanding window cross-validation framework.

Figure A.1: Illustration of expanding window temporal cross-validation[a]



a The dark blue section is the expanding training window, and the light blue section is the corresponding eight-week validation horizon.

Appendix B: Assessment of machine learning model performance by jurisdiction

In this section, we detail the process performed to select the best machine learning model for each state. The models considered are elastic net, support vector, random forest, and feedforward neural network regression models. For easy interpretation of the results presented in this section, we define the following acronyms: MAE: mean absolute error; PCC: Pearson correlation coefficient; PMD: peak magnitude difference; and PWD: peak week difference. These are accuracy measures we applied to assess the predictive performance of the models.

New South Wales: Based on the mean absolute error, the random forest model for one week ahead (MAE: 4.360) and elastic net model for nowcast (MAE: 5.162) predictions, respectively, showed better performance than the rest of the models and prediction types (Figure B.1). These two scenarios produce similar Pearson correlation coefficient values (random forest: 0.959; elastic net: 0.966), but the random forest one-week-ahead model estimated the peak magnitude and its occurrence time more closely (PMD: 2.835; PWD: -2) than did the elastic net model (PMD: -8.903; PWD: 2; Figure B.1). Thus, we chose the random forest one-week ahead prediction as the best scenario.

Victoria: The mean absolute error for support vector (MAE: 6.156), elastic net (MAE: 6.179), and random forest (MAE: 6.348; PCC: 0.934;) models for two-weeks-ahead prediction were all lower than the rest of the scenarios (Figure B.2). The Pearson correlation coefficient for these three scenarios is same (support vector: 0.934; elastic net: 0.934; random forest: 0.934). However, the random forest model predicted the peak magnitude and the time of its occurrence much more closely (PMD: -4.483; PWD: -1) than the support vector (PMD: -12.529; PWD: 3) and elastic net (PMD: -9.860; PWD: 3) models (Figure B.2). As such, the random forest for the two-weeks-ahead scenario was defined as the best model.

Queensland: The mean absolute error for elastic net nowcast (MAE: 7.757) and elastic net one week ahead (MAE: 5.480) scenarios produced better predictive performance than the rest of the scenarios (Figure B.3). These two scenarios produced similar values for the Pearson correlation coefficient (elastic net nowcast: 0.977; elastic net one week ahead: 0.985). Nevertheless, the elastic net nowcast scenario depicted greater accuracy in estimating the peak magnitude (PMD: 5.072; PWD: 2) than the elastic net one-week-ahead scenario (PMD: -16.552; PWD: 2; Figure B3). Consequently, the elastic net model for the nowcast prediction scenario was identified as the best model.

Western Australia: The elastic net nowcast scenario (MAE: 3.278; PCC: 0.907) was the best model (Figure B.4). Though there were other scenarios with lower mean absolute error, the Pearson correlation coefficient for other models was lower than that of the elastic net nowcast scenario (Figure B.4). There was no visible peak in the test set, hence the peak magnitude difference and peak week difference was not computed.

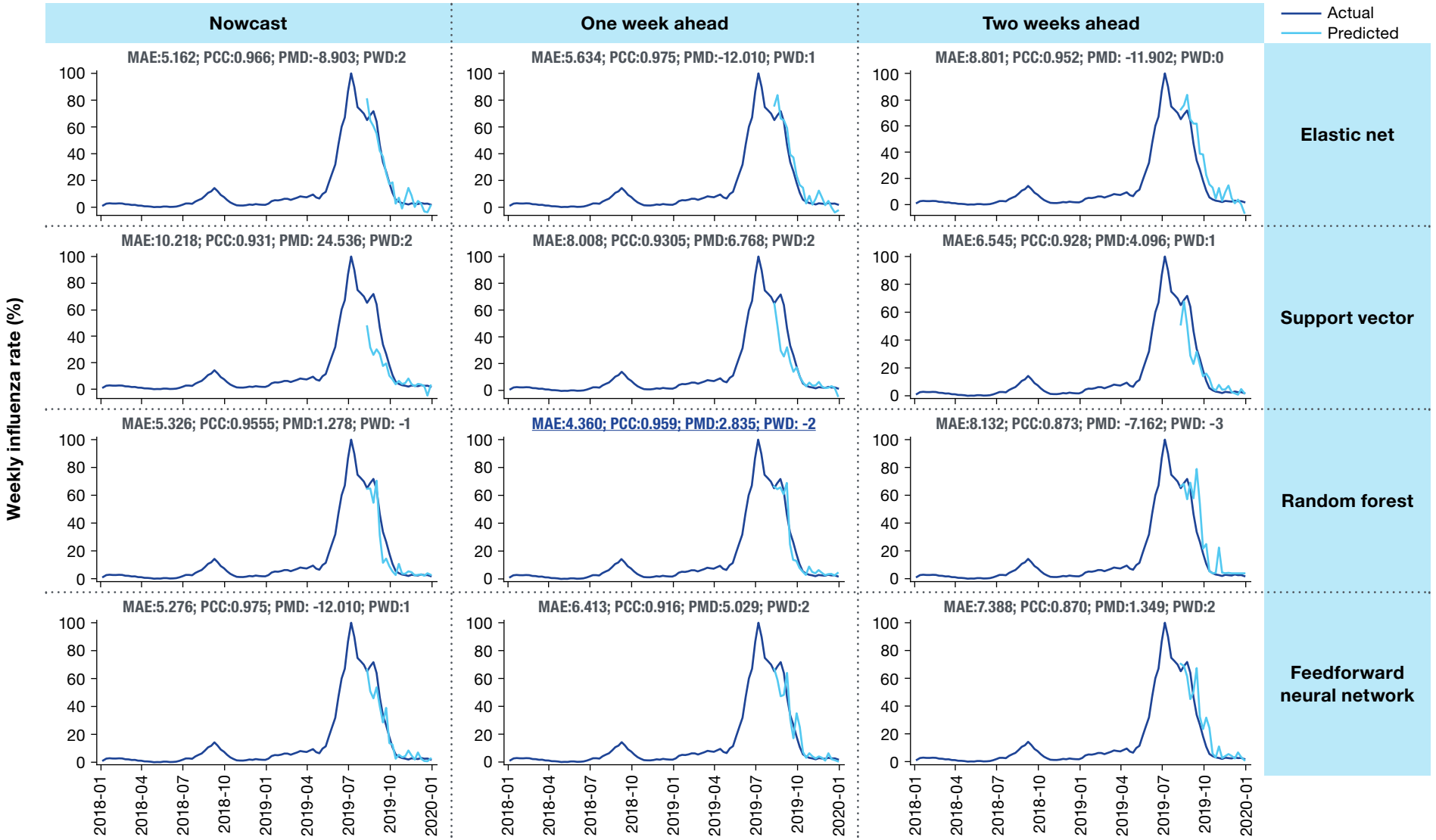
South Australia: The random forest nowcast scenario (MAE: 4.889; PCC: 0.342; PMD: -4.870; PWD: 4) was selected as the best model (Figure B.5). Based on the mean absolute error and Pearson correlation coefficient, the support vector model for the two-weeks-ahead scenario performed similarly (MAE: 4.653; PCC: 0.344; PMD: 4.978; PWD: -5), but its accuracy in predicting the peak magnitude and its timing was less favourable than was the chosen random forest model (Figure B.5).

Northern Territory: In general, the random forest model scenarios only predicted the peaks and peak timing, thus we compared these scenarios. The random forest nowcast scenario (MAE: 7.249; PMD: -9.856; PWD: 6) showed lower MAE than the random forest two-weeks-ahead scenario but was less favourable when estimating the peak magnitude and timing (Figure B.6). Thus, we chose the random forest two-weeks-ahead scenario (MAE: 7.937; PMD: -7.513; PWD: 4) model as the best model (Figure B6). The Pearson correlation coefficient for random forest model scenarios was either not computed, negative, or very low, hence this is not reported in Figure B.6.

Tasmania: The elastic net two-weeks-ahead scenario (MAE: 14.543; PCC: 0.476; PMD: 73.250; PWD: -7) had the lowest MAE but had a similar PCC to that of the random forest two-weeks-ahead scenario (MAE: 16.269; PCC: 0.408; PMD: 54.279; PWD: 0; Figure B.7). Furthermore, the latter model scenario better predicted the peak magnitude and timing. Hence, we selected the random forest model for two weeks ahead prediction as the optimal model.

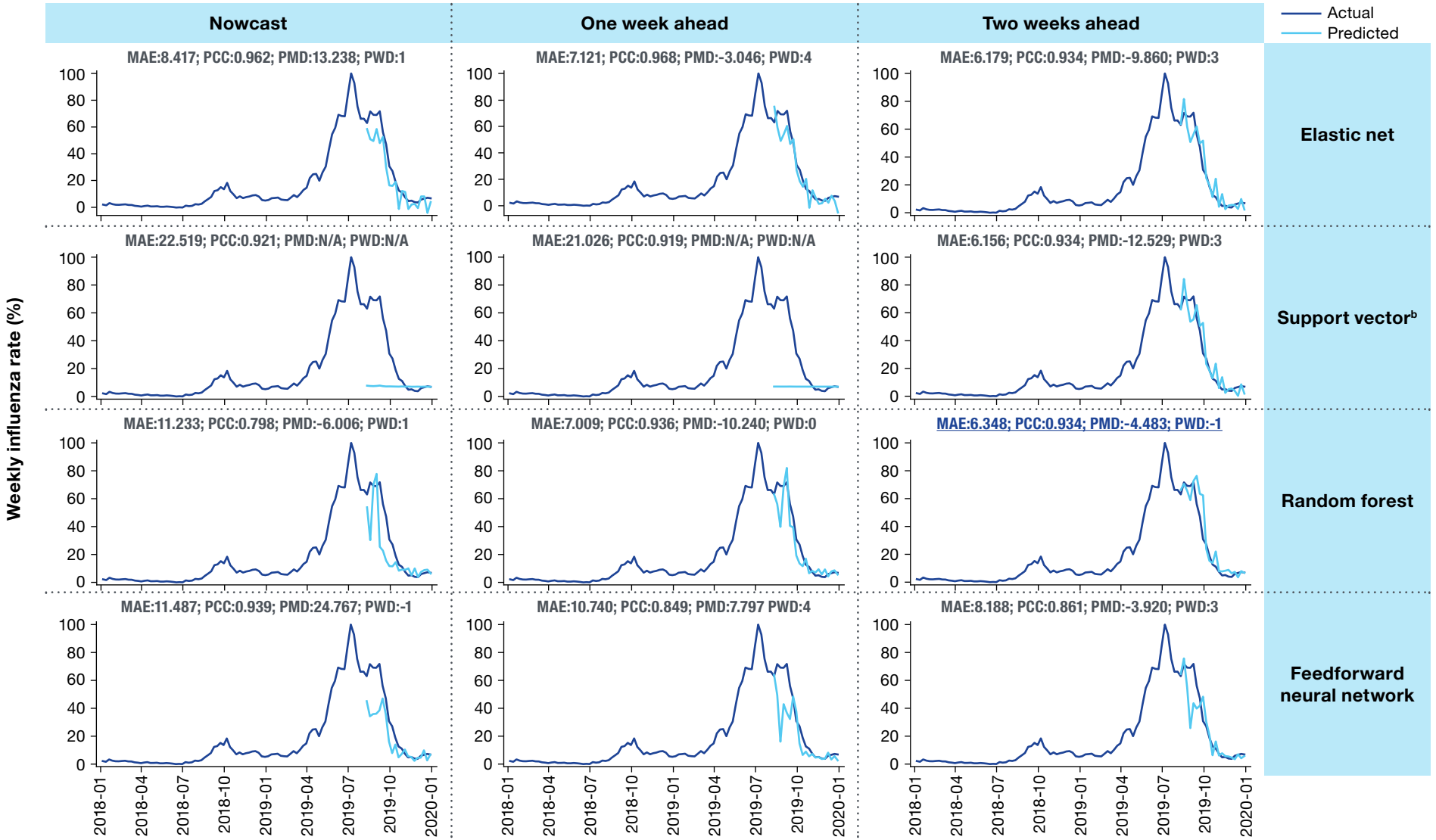
Important keywords: Each state or territory showed different keyword sets as important for predicting influenza rates (Figure B.8). However, the keyword *influenza* was identified as a common keyword in all states and territories.

Figure B.1: Model diagnostics for machine-learning model prediction of scaled weekly influenza rates for New South Wales, Australia,[a] January 2018 – December 2019



a Models employed for influenza rate prediction are elastic net; support vector; random forest; and feedforward neural network. These are assessed for performance, across three prediction types (nowcast, and forecasts one and two weeks ahead) on the basis of mean absolute error (MAE), Pearson correlation coefficient (PCC), peak magnitude difference (PMD), and peak week difference (PWD). Accuracy measures for the best performing of the 12 scenarios are displayed in underlined dark blue.

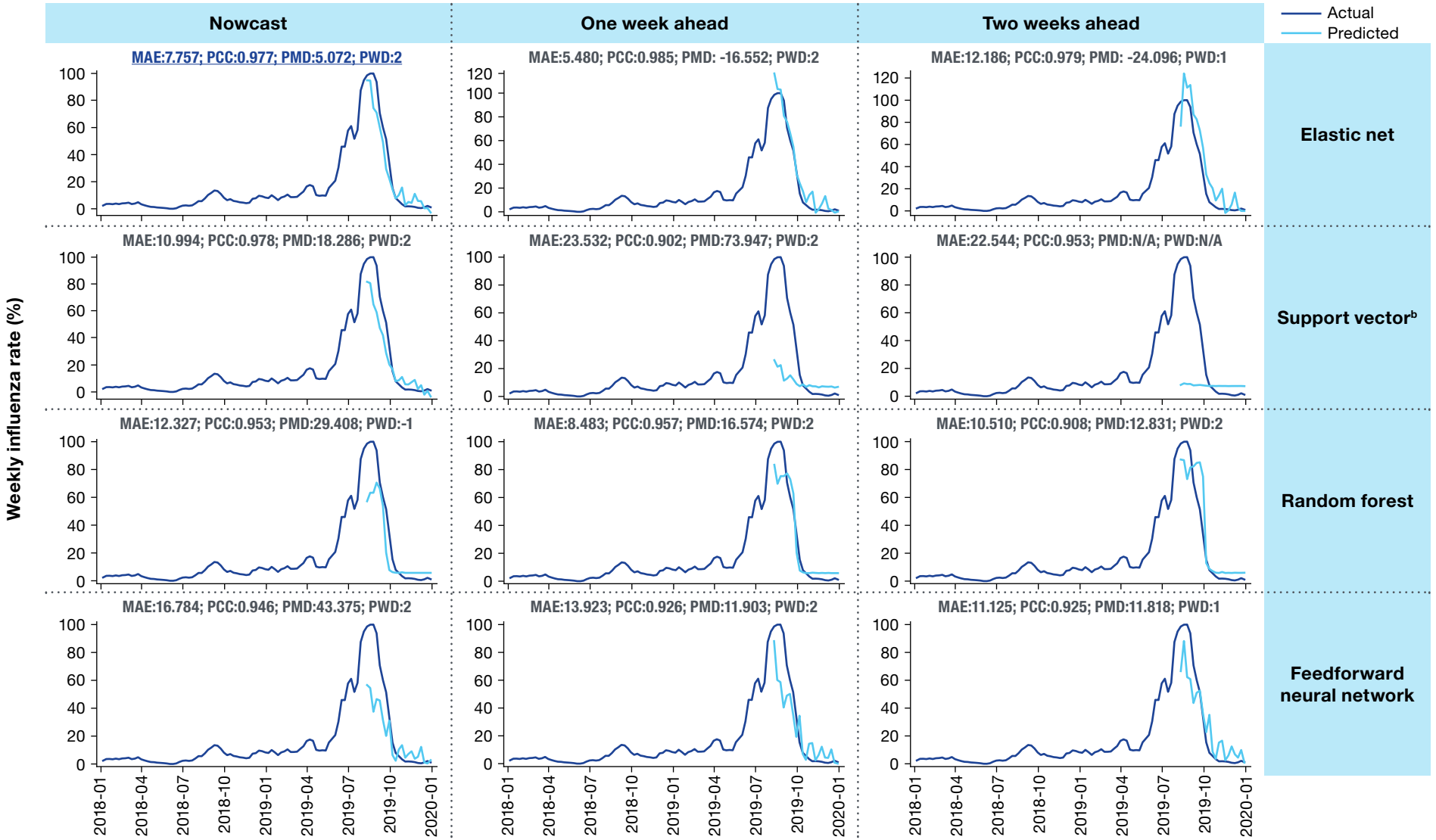
Figure B.2: Model diagnostics for machine-learning model prediction of scaled weekly influenza rates for Victoria, Australia,[a] January 2018 – December 2019



a Models employed for influenza rate prediction are elastic net; support vector; random forest; and feedforward neural network. These are assessed for performance, across three prediction types (nowcast, and forecasts one and two weeks ahead) on the basis of mean absolute error (MAE), Pearson correlation coefficient (PCC), peak magnitude difference (PMD), and peak week difference (PWD). Accuracy measures for the best performing of the 12 scenarios are displayed in underlined dark blue.

b N/A: not applicable, used when there was no peak available for the forecasted period.

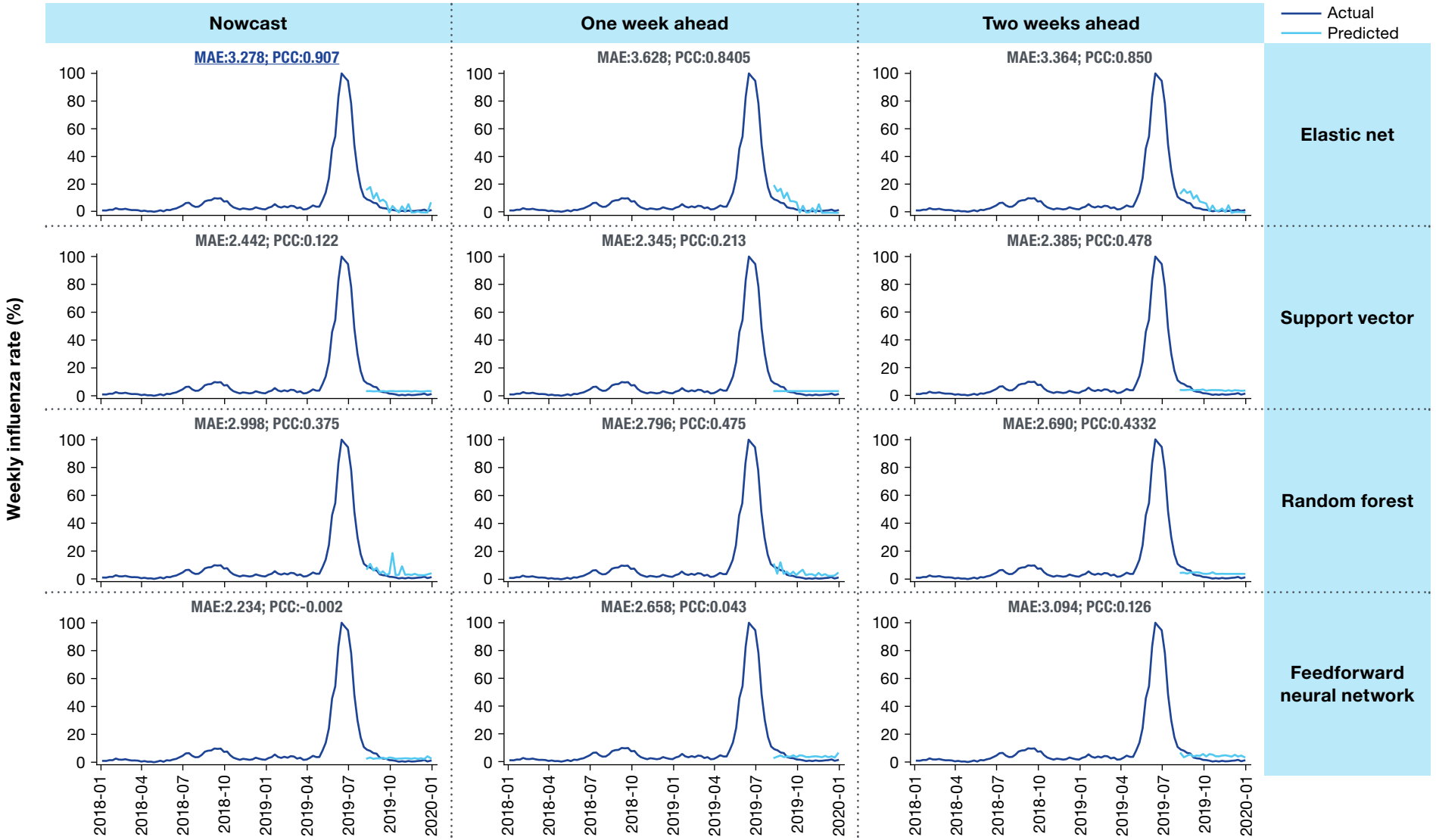
Figure B.3: Model diagnostics for machine-learning model prediction of scaled weekly influenza rates for Queensland, Australia,[a] January 2018 – December 2019



a Models employed for influenza rate prediction are elastic net; support vector; random forest; and feedforward neural network. These are assessed for performance, across three prediction types (nowcast, and forecasts one and two weeks ahead) on the basis of mean absolute error (MAE), Pearson correlation coefficient (PCC), peak magnitude difference (PMD), and peak week difference (PWD). Accuracy measures for the best performing of the 12 scenarios are displayed in underlined dark blue.

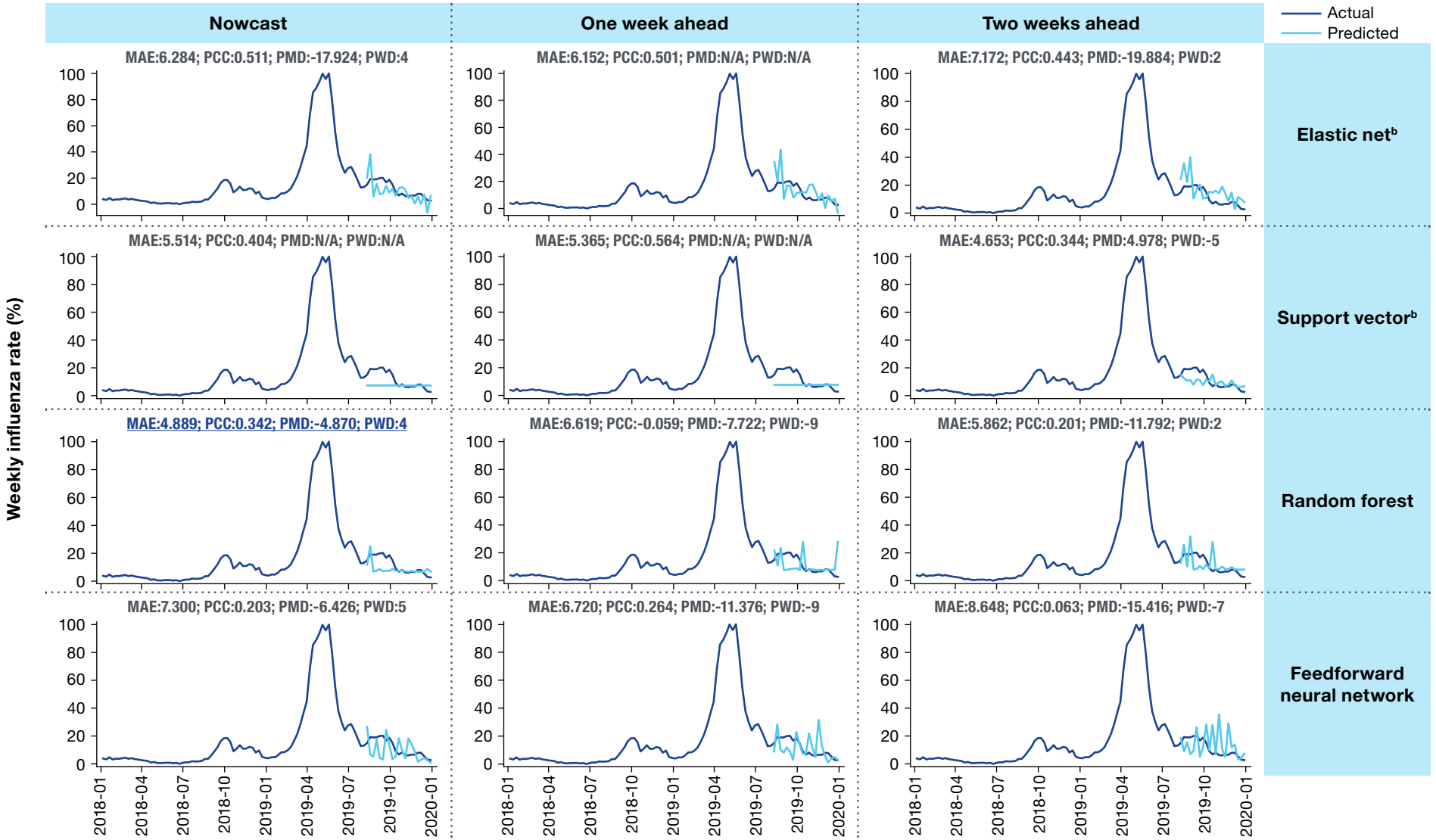
b N/A: not applicable, used when there was no peak available for the forecasted period.

Figure B.4: Model diagnostics for machine-learning model prediction of scaled weekly influenza rates for Western Australia, Australia,[a] January 2018 – December 2019



a Models employed for influenza rate prediction are elastic net; support vector; random forest; and feedforward neural network. These are assessed for performance, across three prediction types (nowcast, and forecasts one and two weeks ahead) on the basis of mean absolute error (MAE) and Pearson correlation coefficient (PCC). Accuracy measures for the best performing of the 12 scenarios are displayed in underlined dark blue.

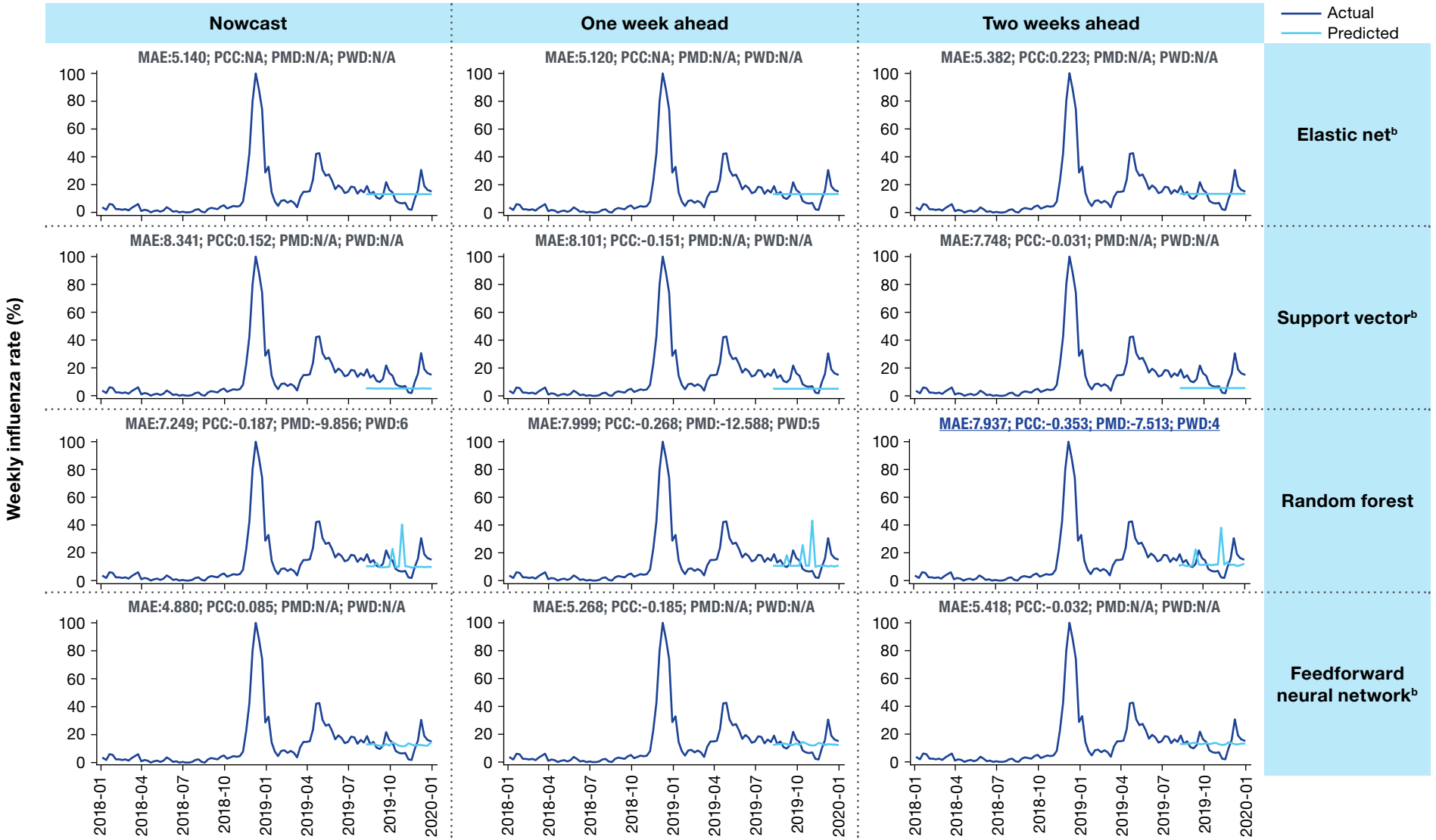
Figure B.5: Model diagnostics for machine-learning model prediction of scaled weekly influenza rates for South Australia, Australia,[a] January 2018 – December 2019



a Models employed for influenza rate prediction are elastic net; support vector; random forest; and feedforward neural network. These are assessed for performance, across three prediction types (nowcast, and forecasts one and two weeks ahead) on the basis of mean absolute error (MAE), Pearson correlation coefficient (PCC), peak magnitude difference (PMD), and peak week difference (PWD). Accuracy measures for the best performing of the 12 scenarios are displayed in underlined dark blue.

b N/A: not applicable, used when there was no peak available for the forecasted period.

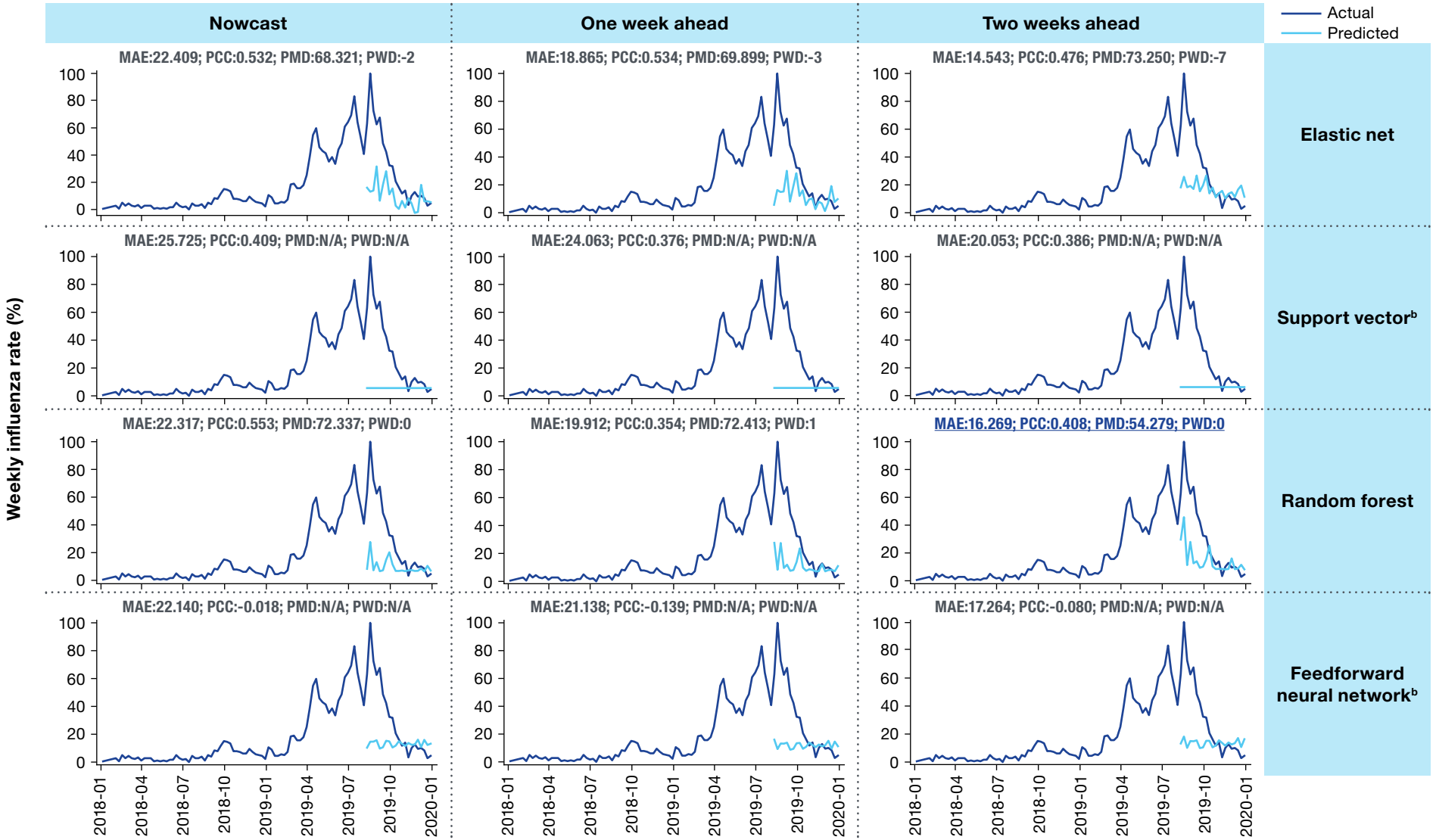
Figure B.6: Model diagnostics for machine-learning model prediction of scaled weekly influenza rates for the Northern Territory, Australia,[a] January 2018 – December 2019



a Models employed for influenza rate prediction are elastic net; support vector; random forest; and feedforward neural network. These are assessed for performance, across three prediction types (nowcast, and forecasts one and two weeks ahead) on the basis of mean absolute error (MAE), Pearson correlation coefficient (PCC), peak magnitude difference (PMD), and peak week difference (PWD). Accuracy measures for the best performing of the 12 scenarios are displayed in underlined dark blue.

b N/A: not applicable, used when there was no peak available for the forecasted period.

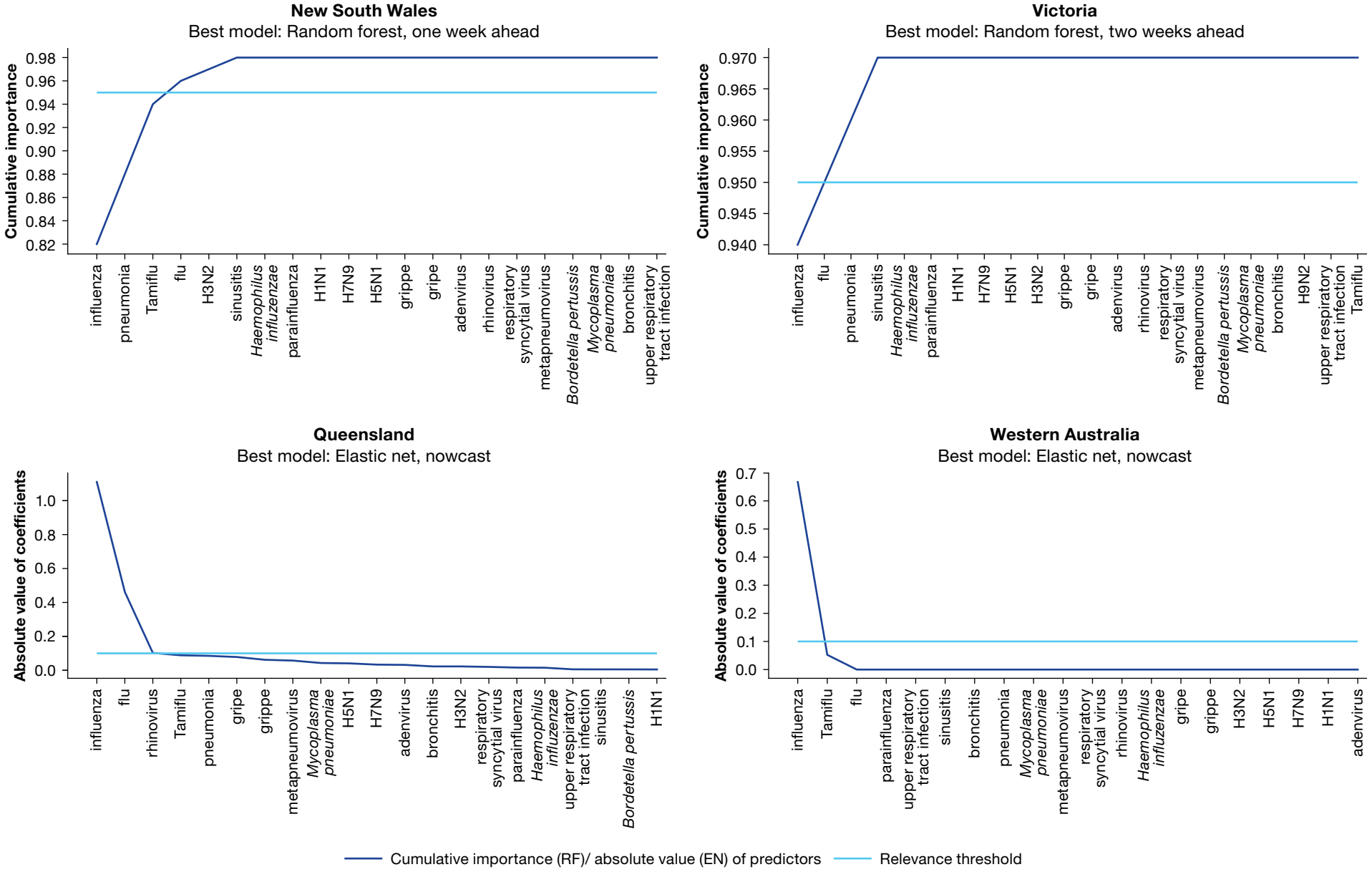
Figure B.7: Model diagnostics for machine-learning model prediction of scaled weekly influenza rates for Tasmania, Australia,[a] January 2018 – December 2019

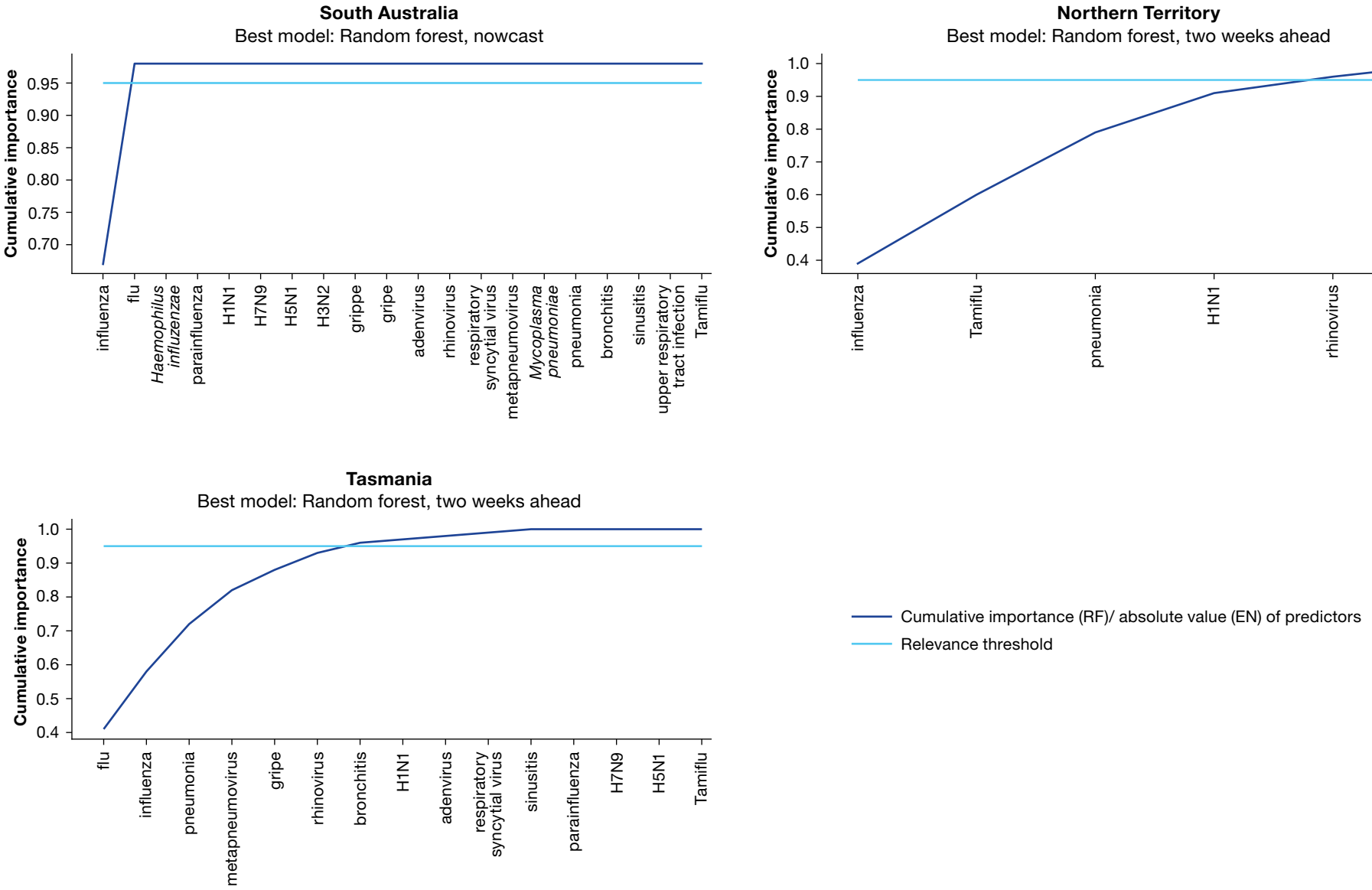


a Models employed for influenza rate prediction are elastic net; support vector; random forest; and feedforward neural network. These are assessed for performance, across three prediction types (nowcast, and forecasts one and two weeks ahead) on the basis of mean absolute error (MAE), Pearson correlation coefficient (PCC), peak magnitude difference (PMD), and peak week difference (PWD). Accuracy measures for the best performing of the 12 scenarios are displayed in underlined dark blue.

b N/A: not applicable, used when there was no peak available for the forecasted period.

Figure B.8: Ranked predictors corresponding to the best model selected for each jurisdiction, for prediction of scaled weekly influenza rates, Australia,[a] January 2018 – December 2019





a Line graphs ranking important predictors for each state and territory from the best model. The cumulative importance curve shows the ranked predictors for the best random forest model. The absolute value of coefficient curve shows the ranked predictors for the best elastic net model. Predictors at and below the blue line are considered relevant for the random forest (RF); those at and above the blue line are considered relevant for the elastic net (EN) models.